Inorganic Chemistry

Article

pubs.acs.org/IC

Nine Diiron(II) Complexes of Three Bis-tetradentate Pyrimidine Based Ligands with NCE (E = S, Se, BH_3) Coligands

Worku A. Gobeze, Victoria A. Milway, Juan Olguín, Guy N. L. Jameson, and Sally Brooker*

Department of Chemistry and the MacDiarmid Institute for Advanced Materials and Nanotechnology, University of Otago, P.O. Box 56, Dunedin 9054, New Zealand

Supporting Information

ABSTRACT: Three bis-*tetra*dentate acyclic amine ligands differing only in the arm length of the pyridine pendant arms attached to the 4,6-positions of the pyrimidine ring, namely, 4,6-bis[*N*,*N*-bis(2′-pyridylethyl)aminomethyl]-2-phenylpyrimidine ($\mathbf{L^{Et}}$), 4,6-bis[*N*,*N*-bis(2′-pyridylmethyl)aminomethyl]-2-phenylpyrimidine ($\mathbf{L^{Me}}$), and 4,6-[(2′-pyridylmethyl)-2′-pyridylethyl)aminomethyl]-2-phenylpyrimidine ($\mathbf{L^{Mix}}$) have been used to synthesize nine air-sensitive diiron(II) complexes: $[Fe^{II}_2\mathbf{L^{Et}}(NCS)_4]\cdot MeOH\cdot{}^3/_4H_2O$ (**1**·MeOH·$^3/_4H_2O$), $[Fe^{II}_2\mathbf{L^{Et}}(NCSe)_4]\cdot H_2O$ (**2**·H_2O), $[Fe^{II}_2\mathbf{L^{Et}}(NCBH_3)_4]\cdot{}^5/_2H_2O$ (**3**·$^5/_2H_2O$), $[Fe^{II}_2\mathbf{L^{Me}}(NCS)_4]\cdot{}^1/_2H_2O$ (**4**·$^1/_2H_2O$), $[Fe^{II}_2\mathbf{L^{Me}}(NCSe)_4]$ (**5**), $[Fe^{II}_2\mathbf{L^{Me}}(NCBH_3)_4]\cdot{}^3/_2H_2O$ (**6**·$^3/_2H_2O$), $[Fe^{II}_2\mathbf{L^{Mix}}(NCS)_4]\cdot{}^1/_2H_2O$ (**7**·$^1/_2H_2O$), $[Fe^{II}_2\mathbf{L^{Mix}}(NCSe)_4]\cdot{}^3/_2H_2O$ (**8**·$^3/_2H_2O$), and $[Fe^{II}_2\mathbf{L^{Mix}}(NCBH_3)_4]\cdot{}^3/_2H_2O$ (**9**·$^3/_2H_2O$). Complexes **3**·$^5/_2H_2O$, **4**·$^1/_2H_2O$, **5**, **6**·$^3/_2H_2O$, and **8**·$^3/_2H_2O$ were structurally characterized by X-ray crystallography, revealing, in all cases, both of the iron(II) centers in an octahedral environment with two NCE (E = S, Se, or BH_3) anions in a cis-position relative to one another. Variable temperature magnetic susceptibility measurements showed that all nine diiron(II) complexes are stabilized in the [HS-HS] state from 300 K to 4 K, and exhibit weak antiferromagnetic coupling. Mössbauer spectroscopy confirmed the spin and oxidation states of eight of the nine complexes (the synthesis of air-sensitive complex **3** was not readily reproduced).

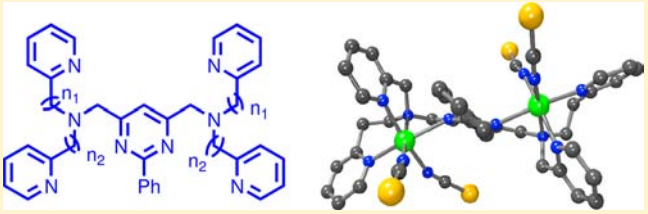

INTRODUCTION

The spin crossover (SCO) field is an area of contemporary coordination chemistry that has driven an increase in reports of the preparation and study of the magnetic properties of iron(II) complexes. Spin crossover occurs when the electronic configuration of the metal ion is switched between the high-spin (HS) and low-spin (LS) states, driven by external stimuli (temperature, pressure, light irradiation, or magnetic field). When the SCO effect is accompanied by hysteresis it confers a memory effect which makes these materials potential candidates for information storage and other molecular devices.[1,2]

One of the interests of this research group is the synthesis and design of dinucleating ligands that upon coordination to iron(II)[3,4] or cobalt(II)[5] centers may lead to observation of SCO and magnetic coupling. We have previously reported the synthesis of the bis-*ter*dentate-triazole based **PMAT** ligand[6] (Figure 1) and its diiron(II) complex, $[Fe^{II}_2(\mathbf{PMAT})_2](BF_4)_4$·DMF, in which two ligand strands fully encapsulate two metal centers, with all 12 donors coming from just the two ligand strands. The SCO properties of this complex are unique. The localized [HS-LS] state is stable over a very wide range of temperatures, with spin transition (ST) to the [HS-HS] form occurring at $T_{1/2}$ = 225 K[3,4] and no evidence of a second ST to the [LS-LS] form, even under 10.3 Kbar at 4 K.[7] That study was extended to include consideration of the effect the choice of counteranion X, in $[Fe^{II}_2(\mathbf{PMAT})_2](X)_4$·solvents, has on the SCO behavior.[8]

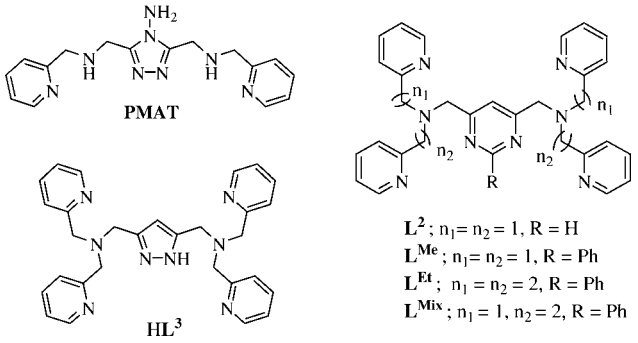

Figure 1. Schematic representation of the literature bis-*ter*dentate **PMAT** ligand and bis-*tetra*dentate $\mathbf{L^2}$ and $\mathbf{HL^3}$ ligands used for the generation of dinuclear iron(II) complexes, and the ligands synthesized in this work, $\mathbf{L^{Et}}$, $\mathbf{L^{Me}}$, and $\mathbf{L^{Mix}}$, from which nine dinuclear iron(II) complexes are made.

More recently we have moved from bis-*ter*dentate ligands to various bis-*tetra*dentate ligands, as the latter allow us to generate diiron(II) complexes in which only one ligand strand coordinates to the two metal centers, leaving the six-coordination of each iron(II) ion to be completed by N-

Received: June 6, 2012
Published: July 27, 2012

   dx.doi.org/10.1021/ic3012052 | *Inorg. Chem.* 2012, 51, 9056−9065

based anions such as NCE (E = S, Se, BH_3). To the best of our knowledge, only two examples of dinucleating bis-*tetra*dentate ligands have been used before in the preparation of diiron(II) complexes with N-based anions. One of them is a pyrazole-based ligand, HL^3 (Figure 1), deprotonated and used to generate two diiron(II) complexes by this research group,[9] namely, the K^+ salt of anionic symmetric $[Fe^{II}_2(L^3)(NCS)_4]^-$ and the neutral asymmetric $[Fe^{II}_2(L^3)(py)(SeCN)(NCSe)_2]$, both stabilized in the [HS-LS] state in the 300−2 K temperature range. The second example is a pyrimidine-based ligand, L^2 (Figure 1), reported by Oshio and Ichida,[10] which was used to generate the neutral, symmetrical dinuclear iron(II) complex $[Fe^{II}_2(L^2)(NCS)_4]$. X-ray analysis and variable temperature magnetic susceptibility measurements showed that the iron(II) centers are stabilized in the HS state at all temperatures with a fairly weak antiferromagnetic coupling between them (Curie and Weiss constants: C = 3.77 emu atom^{-1} K and θ = −3.86 K, for data 100−270 K).

A significant number of iron(II) complexes of pyrimidine-based ligands have shown SCO behavior.[11−18] Hence we decided to study the iron(II) coordination chemistry of three ligands very similar to L^2, but featuring a phenyl substituent, not a hydrogen atom as in L^2, at the 2-position of the pyrimidine ring (Figure 1). The three phenyl-substituted ligands, namely, 4,6-bis[*N*,*N*-bis(2′-pyridylethyl)-aminomethyl]-2-phenylpyrimidine (L^{Et}),[19] 4,6-bis[*N*,*N*-bis(2′-pyridylmethyl)aminomethyl]-2-phenylpyrimidine (L^{Me}), and 4,6-[(2′-pyridylmethyl)-2′-pyridylethyl)aminomethyl]-2-phenylpyrimidine (L^{Mix}), provide differing alkyl chain lengths between the pyridine moieties and the pyrimidine ring (Figure 1), and hence generate differing combinations of chelate ring sizes (and variations in strain) when bound to the metal ions. The phenyl substituent was introduced primarily because of our well established access to the required precursor, along with the expectation that it should enhance the solubility of both the ligand and the resulting complexes in organic solvents, and perhaps also the ease of crystallization. It should also be noted that the bulky phenyl substituent inductively withdraws electron density from the pyrimidine ring, reducing its basicity. Hence the ligand field imposed by L^{Me} is expected to be different, probably somewhat lower, than that of L^2, as seen in the substituent study carried out by Lehn and co-workers on a series of tetranuclear iron(II) pyrimidine-based grid complexes (phenyl, SCO-active; hydrogen, fully LS).[15,20] The differing alkyl "arm" lengths offer further variations in the ligand field strength, the general principle of which is established in the literature.[21−23] The effect of the choice of NCE (E = S, Se, and BH_3)[24−27] coligands is also considered here, as this is a particularly powerful way to control the field strength about the iron(II) centers. Herein we report the synthesis, structural characterization, magnetic and Mossbauer study of nine iron(II) complexes derived from the three bis-*tetra*dentate ligands, L^{Et}, L^{Me}, and L^{Mix}.

RESULTS AND DISCUSSION

Organic Synthesis. We previously reported the synthesis of bis(hydroxymethyl)-2-phenylpyrimidine (**A**), 4,6-bis-(aminomethyl)-2-phenylpyrimidine (**B**), and L^{Et}.[19] Dialcohol **A** was converted to 4,6-bis(chloromethyl)-2-phenylpyrimidine (**C**) by addition of 2 equivalents of $SOCl_2$ to a yellow dichloromethane solution of **A** under an inert atmosphere (N_2 or Ar; NB. This reaction does not work when done in air). After the deep yellow suspension was stirred for 1 h, it was taken to dryness by blowing nitrogen gas over it, to give **C** as a pure yellow solid in a quantitative yield. Finally, nucleophilic substitution reactions of **C** with either *N*-bis(2-pyridylmethyl)-amine (**bmpa**)[28,29] or *N*-(2-pyridylethyl)-*N*-(2′-pyridylmethyl)-amine (**pmpea**)[30,31] gave L^{Me} and L^{Mix}, in 95 and 75% yield, respectively (Scheme 1).

Scheme 1[a]

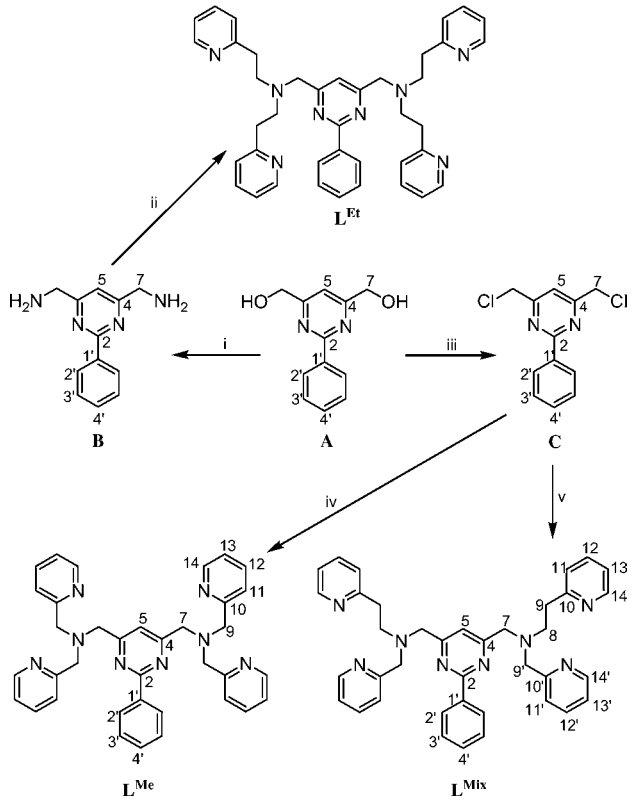

[a](i) (a) PPh_3, Phthalimide, DIAD, THF, rt; (b) H_2N-NH_2·H_2O, EtOH, rt; (ii) vinylpyridine, MeOH, ACOH, reflux, 1 week; (iii) $SOCl_2$, CH_2Cl_2, N_2; (iv) **bmpa**[28,29] (2 equiv.), Na_2CO_3, MeCN, KI, reflux; (v) **pmpea**[30,31] (2 equiv.), Na_2CO_3, MeCN, KI, reflux.

Complex Synthesis. All three ligands, L^{Et}, L^{Me}, and L^{Mix} generate air-sensitive iron(II) complexes. Thus, all of the complexation reactions were carried out under an inert atmosphere (argon or nitrogen) from 1 equivalents of the appropriate ligand and 2 equivalents of freshly prepared $[Fe^{II}(NCE)_2(py)_4]$, E = S, Se, or BH_3, at reflux. The latter starting materials[32] were chosen as a source of iron(II) and NCE coligands, and are shown here to be labile enough to allow stoichiometry controlled formation of the desired products.

Either methanol or acetonitrile was used as the reaction solvent (Table 1). Methanol was used for all but four complexes, the NCS-containing $4{\cdot}^1/_2H_2O$ and the $NCBH_3$-based $3{\cdot}^5/_2H_2O$, $6{\cdot}^3/_2H_2O$, and $9{\cdot}H_2O$ (MeCN used). For those four exceptions, although inert conditions were employed, clean product could not be obtained reproducibly from MeOH. In most of the cases the microanalytical results gave much lower values than expected, probably because of ferric impurities. Oxidation of iron(II) complexes in methanol even under an inert atmosphere has been observed before when the iron(II) is bound to amine nitrogen donor atom rich

dx.doi.org/10.1021/ic3012052 | Inorg. Chem. 2012, 51, 9056−9065

Table 1. Summary of the Percentage Yield, Color, Solvent Used, "Bulk" Product Isolation, and Crystallization Methods for $[Fe^{II}_2L^{Et}(NCS)_4]\cdot MeOH\cdot{}^3/_4H_2O$ ($1\cdot MeOH\cdot{}^3/_4H_2O$**), $[Fe^{II}_2L^{Et}(NCSe)_4]\cdot H_2O$ (**$2\cdot H_2O$**), $[Fe^{II}_2L^{Et}(NCBH_3)_4]\cdot{}^5/_2H_2O$ (**$3\cdot{}^5/_2H_2O$**), $[Fe^{II}_2L^{Me}(NCS)_4]\cdot{}^1/_2H_2O$ (**$4\cdot{}^1/_2H_2O$**), $[Fe^{II}_2L^{Me}(NCSe)_4]$ (**5**), $[Fe^{II}_2L^{Me}(NCBH_3)_4]\cdot{}^3/_2H_2O$ (**$6\cdot{}^3/_2H_2O$**), $[Fe^{II}_2L^{Mix}(NCS)_4]\cdot{}^1/_2H_2O$ (**$7\cdot{}^1/_2H_2O$**), $[Fe^{II}_2L^{Mix}(NCSe)_4]\cdot{}^3/_2H_2O$ (**$8\cdot{}^3/_2H_2O$**) and $[Fe^{II}_2L^{Mix}(NCBH_3)_4]\cdot{}^3/_2H_2O$ (**$9\cdot{}^3/_2H_2O$**)**

								IR[d]	
ligand	complex	co-ligand	yield[a]	color	solvent	isolation method[b]	crystallization method[c]	N≡C	B–H
L^{Et}	$1\cdot MeOH\cdot{}^3/_4H_2O$	NCS	80	orange	MeOH	A		2038	
	$2\cdot H_2O$	NCSe	85	yellow	MeOH	A		2061	
	$3\cdot{}^5/_2H_2O$	$NCBH_3$	91	yellow	MeCN	A	VD	2182	2334
L^{Me}	$4\cdot{}^1/_2H_2O$	NCS	80	brick red	MeCN	B	LLD1	2068	
	5	NCSe	82	brick red	MeOH	B	LLD1	2053	
	$6\cdot{}^3/_2H_2O$	$NCBH_3$	92	orange	MeCN	A	LLD1	2177	2339
L^{Mix}	$7\cdot{}^1/_2H_2O$	NCS	58	yellow	MeOH	B		2068	
	$8\cdot{}^3/_2H_2O$	NCSe	79	yellow	MeOH	B	LLD2	2064	
	$9\cdot{}^3/_2H_2O$	$NCBH_3$	90	yellow	MeCN	A		2187	2334

[a]units %. [b]A = Et_2O addition to reaction solution; B = precipitated from the reaction solution. [c]VD = vapor diffusion of Et_2O into DMF:MeCN (1:5) solution; LLD1 = liquid–liquid diffusion in an H-tube in MeOH; LLD2 = liquid–liquid diffusion in an H-tube in MeOH-EtOH (2:1). [d]units cm^{-1}.

ligands that enhance the basic character and stabilize iron(III).[33]

Four of the complexes, $4\cdot{}^1/_2H_2O$, **5**, $7\cdot{}^1/_2H_2O$, and $8\cdot{}^3/_2H_2O$, precipitated directly from the reaction solution (Table 1), so were simply filtered off. The other five complexes did not precipitate, so initially the reaction solutions were vapor diffused with diethyl ether, under Schlenk conditions. However, this resulted in solids for which variable and poor microanalysis data were obtained, again presumably because of partial oxidation to ferric products. Therefore the isolation of these five complexes, namely, $1\cdot MeOH\cdot{}^3/_4H_2O$, $2\cdot H_2O$, $3\cdot{}^5/_2H_2O$, $6\cdot{}^3/_2H_2O$, and $9\cdot H_2O$, was instead achieved by slow addition of diethyl ether by cannula into the reaction solution (Table 1). Only in the case of **3** was even this method found not to be totally reliable (see later).

This resulted in nine complexes, in 58–92% yield. In all cases the microanalysis and electrospray ionization mass spectrometry (ESI-MS) results were consistent with those expected for the desired dinuclear complexes. This was confirmed by X-ray crystallography for $3\cdot{}^5/_2H_2O$, $4\cdot{}^1/_2H_2O$, **5**, $6\cdot{}^3/_2H_2O$, and $8\cdot{}^3/_2H_2O$ (see below). A summary of the yields, colors, reaction solvents, "bulk" product isolation methods, crystallization methods, and IR stretches for the coligands, is presented in Table 1.

IR Study of Complexes. For complexes which contain NCE anions, the position of the C≡N stretch provides useful information with regard to the spin state of the iron(II) center. For E = S and Se:[34] 2020–2080 cm^{-1} for HS iron(II)[11,27,35] vs ~2100 cm^{-1} for N-bound LS iron(II).[36] Further, for NCS and NCSe complexes the position of the C≡N stretch helps to identify the binding mode of the anions: 2020–2080 cm^{-1} indicates N-bound while bands higher than ~2100 cm^{-1} indicate S-bound or Se-bound (Table 1).[37,38] For $NCBH_3$ complexes the C≡N stretch always shows up higher than ~2100 cm^{-1} when N-bound, and a strong B–H stretch occurs at ~2300 cm^{-1}.[27,39–41]

The C≡N stretches for the six present E = S and Se complexes, $1\cdot MeOH\cdot{}^3/_4H_2O$, $2\cdot H_2O$, $4\cdot{}^1/_2H_2O$, **5**, $7\cdot{}^1/_2H_2O$, and $8\cdot{}^3/_2H_2O$, occurred as a single band in the range 2039–2062 cm^{-1}, consistent with them all being N-bound, as expected (Table 1).[37] This is also indicative of all of these complexes being [HS-HS] at room temperature. The C≡N stretch for the three E = BH_3 complexes, $3\cdot{}^5/_2H_2O$, $6\cdot{}^3/_2H_2O$, and $9\cdot H_2O$, was observed at 2185, 2179, and 2173 cm^{-1}, respectively (B–H stretch at 2342, 2347, and 2342 cm^{-1}, respectively), as expected for N-bound $NCBH_3$.

X-ray Crystal Structures. Single crystals of $3\cdot{}^5/_2H_2O$ and $6\cdot{}^3/_2H_2O$ were obtained as $3\cdot DMF\cdot MeCN\cdot{}^3/_5Et_2O$ (yellow) and solvent free **6** (orange) by diethyl ether diffusion into the MeCN:DMF (5:1) and MeCN solutions of the complexes, respectively, while $4\cdot{}^1/_2H_2O$ and $8\cdot{}^3/_2H_2O$ were obtained as solvent free **4** (red), and $8\cdot{}^7/_{10}MeOH$ (orange-red), by liquid–liquid diffusion of the ligand and the appropriate $[Fe^{II}(NCE)_2(py)_4]$ in MeOH and MeOH-EtOH (2:1) mixture of solvents, respectively (Table 1 and Supporting Information, Table S1). Single crystals of **5** (orange-red) were also obtained solvent free by liquid–liquid diffusion of the ligand and $[Fe^{II}(NCBH_3)_2(py)_4]$ in MeOH.

Complex $3\cdot DMF\cdot MeCN\cdot{}^3/_5Et_2O$ crystallized in the *Pnma* space group with half of the molecule in the asymmetric unit (Figure 2) and the other half generated by a mirror plane through the C2 and C4 atoms of the pyrimidine ring and the entire phenyl ring. The set of iso-structural complexes **4**–**6** (Figure 3, Supporting Information, Figure S2 and S4) which crystallized in the $P2_1/n$ space group, and complex

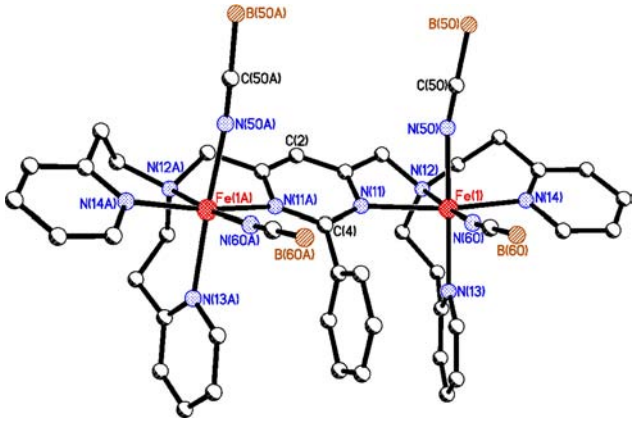

Figure 2. View of the molecular structure of $[Fe^{II}_2L^{Et}(NCBH_3)_4]$ of $3\cdot DMF\cdot MeCN\cdot{}^3/_5Et_2O$. Hydrogen atoms and solvent molecules have been omitted for clarity. Symmetry operation A is x, $3/2 - y$, z.

dx.doi.org/10.1021/ic3012052 | Inorg. Chem. 2012, 51, 9056–9065

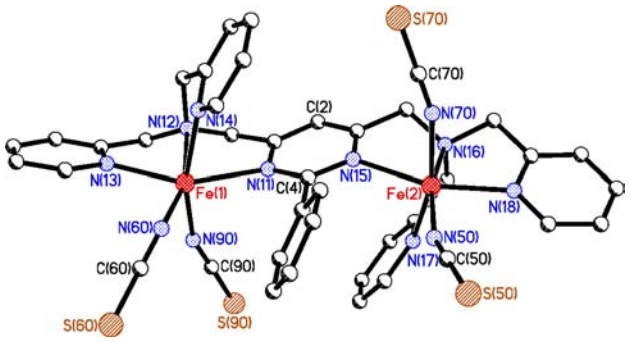

Figure 3. View of the molecular structure of $[Fe^{II}_2L^{Me}(NCS)_4]$ **4**. Hydrogen atoms have been omitted for clarity.

8·$^{7}/_{10}$MeOH (Figure 4) which crystallized in the $P2_1/c$ space group, all have the entire molecule in the asymmetric unit.

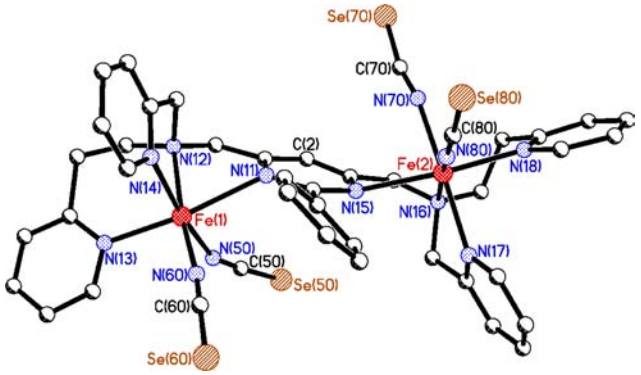

Figure 4. View of the molecular structure of $[Fe^{II}_2L^{Mix}(NCSe)_4]$ of **8**·$^{7}/_{10}$MeOH. Hydrogen atoms and solvent molecules have been omitted for clarity.

In all cases the ligands are bound in a bis-*tetra*dentate fashion via the nitrogen atoms of the pyrimidine ring (N_{pym}), tertiary amine (N_{amine}), and the two pyridine rings ($2N_{py}$). Two NCE coligands ($2N_{NCE}$) in *cis* positions complete the octahedral (Oh) geometry (N_6 mode) around each iron(II) ion. To give a common reference point we define the "axial" direction in these complexes to lie along the weak Fe–N_{pym} bond and one of the two N_{py} bonds (the one that is *trans* to N_{pym}), while the "equatorial" plane comprises the other N_{py}, N_{amine}, and two *cis*-positioned NCE coligands. The Fe–N_{NCE} bonds are the shortest, consistent with literature reports of related complexes,[10,18,42] while the Fe–N_{pym} bonds are the longest, presumably because of the weak basic nature of the phenyl-substituted (inductively electron withdrawing) pyrimidine ring relative to the pyridine ring and the tertiary amine. The mean Fe–N bond distances (Table 2, 2.182–2.200 Å) are entirely consistent with the iron(II) centers being in the HS state at 91–92 K.[3,43] The individual *cis*–N–Fe–N [70.4(2)–120.8(2)°] and *trans*–N–Fe–N [148.8(2)–176.7(2)°] bond angles in these five dimetallic structures are widely dispersed (Table 2), which is also consistent with HS centers. Nevertheless, the average *cis* angles (89.7–90.0°) are remarkably close to a perfect 90° as expected for ideal octahedral geometries observed in contrast to the widely dispersed *trans* angles (average *trans* angles 157.9–171.9°).

In the complex of the all-ethylene-armed ligand, **3**·DMF·MeCN·$^{3}/_{5}$Et$_2$O, the Fe1···Fe1A distance across the pyrimidine bridge is 6.626(2) Å (Table 2), with the iron atoms displaced from the pyrimidine mean plane by 0.556 Å. The octahedral distortion parameter Σ value (Σ is defined as the sum of the deviation of each of the 12 *cis*-angles associated with the iron(II) center)[44,45] is 50.1°, the smallest deviation from ideal geometry in this family of complexes (Table 2). Because of symmetry, the pyrimidine ring is perfectly orthogonal to the attached phenyl ring, and almost parallel to the axially positioned pyridine ring, intersecting at only 7.2(3)°. The N–C–B groups are almost linear [178.4(5)–179.2(6)°] while the Fe–N–C(B) linkage is slightly bent [167.3(4)–173.9(4)°].

In the three iso-structural complexes of the all-methylene-armed ligand, **4**, **5**, and **6** (Figure 3, Supporting Information, Figures S2 and S4, Table 2), the Fe···Fe distance across the pyrimidine bridge is 6.563(2), 6.574(1), and 6.526(1) Å, respectively. A shorter Fe···Fe separation [6.288(1) Å] was reported for $[Fe^{II}_2(L^2)(NCS)_4]$,[10] consistent with the report of a shorter Fe–N_{pym} bond (2.229 Å) than is seen in **4**–**6** (Table 2, 2.288–2.299 Å). The Fe(1) and Fe(2) centers in **4**–**6** are significantly displaced above and below the pyrimidine mean plane (**4**: 0.482, −0.531; **5**: 0.491, −0.502, **6**: 0.510, −0.524 Å). The distortion parameters for **4**–**6** (Σ = 102.8–118.4°) are larger than for **3**·DMF·MeCN·$^{3}/_{5}$Et$_2$O (50.1°). The N–C–S, N–C–Se, and N–C–BH_3 groups are almost linear [**4**: 176.7(8)–179.5(8); **5**: 176.9(6)–178.3(6); **6**: 177.2(7)–179.6(7)°] while the Fe–N–C(S), Fe–N–C(Se), and Fe–N–C(BH_3) linkages are significantly bent [**4**: 144.7(7)–161.9(6); **5**: 149.4(5)–162.5(5); **6**: 153.1(5)–168.8(5)°]. The phenyl ring is tilted out of the plane of the attached pyrimidine ring by 53.2(2), 54.5(1), and 59.2(1)° for **4**–**6**, respectively.

The Fe···Fe distance across the pyrimidine bridge in the complex of the mixed-ethylene-methylene-armed ligand, **8**·$^{7}/_{10}$MeOH (Figure 4), is 6.782(1) Å, and is the longest observed in this family (Table 2). This is consistent with this complex also featuring the longest Fe–N_{pym} bonds (average 2.391 Å, Table 2) and the biggest displacement of the iron centers from the pyrimidine ring plane (1.106 and −1.325 Å). Interestingly, the degree of deviation from octahedral geometry (mean Σ = 80.6°) for this complex of the L^{Mix} ligand, **8**·$^{7}/_{10}$MeOH, lies between the value seen for the complex of the L^{Et} ligand, **3**·DMF·MeCN·$^{3}/_{5}$Et$_2$O (50.1°), and those seen in the complexes of the L^{Me} ligand, **4**–**6** (102.8–118.4°). The phenyl ring is twisted away from the pyrimidine mean plane by 33.5(3)°. As for **5**, the N–C–Se groups are almost linear [176.0(1)–179.3(8)°] while the Fe–N–C(Se) linkages are somewhat bent [158.1(8)–171.5(7)°]. A hydrogen bond is present between the methanol molecule in the lattice and the coordinated selenocyanate counteranion (Supporting Information, Table S7).

Comparisons of Structures. An interesting difference between these structures is in the position of the pyridyl and NCE groups relative to one another. In **3**·DMF·MeCN·$^{3}/_{5}$Et$_2$O each pair of "*cis*" positioned NCE anions that are symmetry related bind from the same side, so are considered to be "*cis*" relative to one another while in **8**·$^{7}/_{10}$MeOH they are "*trans*" relative to one another. However, in **4**–**6** the pairs of NCE anions are neither "*cis*" nor "*trans*" to one another. Rather, one NCE on each iron(II) center is *cis* to an NCE on the other iron(II) center, while the "other" NCE is *trans* to the other NCE anion. The equatorial pyridine rings in **3**·DMF·MeCN·$^{3}/_{5}$Et$_2$O are "*cis*" relative to one another, while in the other four structures they are "*trans*" relative to one another.

dx.doi.org/10.1021/ic3012052 | *Inorg. Chem.* 2012, 51, 9056–9065

Table 2. Selected Bond Lengths, Angles, and M···M Separation for $[Fe^{II}_2L^{Et}(NCBH_3)_4]\cdot DMF\cdot MeCN\cdot{}^3/_5Et_2O$ (3·DMF·MeCN·$^3/_5Et_2O$), $[Fe^{II}_2L^{Me}(NCS)_4]$ (4), $[Fe^{II}_2L^{Me}(NCSe)_4]$ (5), $[Fe^{II}_2L^{Me}(NCBH_3)_4]$ (6), $[Fe^{II}_2L^{Mix}(NCSe)_4]\cdot{}^7/_{10}MeOH$ (8·$^7/_{10}$MeOH)

	complex				
	$[Fe^{II}_2L^{Et}(NCBH_3)_4]\cdot$solvents	$[Fe^{II}_2L^{Me}(NCS)_4]$	$[Fe^{II}_2L^{Me}(NCSe)_4]$	$[Fe^{II}_2L^{Me}(NCBH_3)_4]$	$[Fe^{II}_2L^{Mix}(NCSe)_4]\cdot{}^7/_{10}MeOH$
Fe−N_{NCE} (Å) (mean)	2.112(4), 2.164(5) (2.138)	2.025(7)−2.115(7) (2.068)	2.023(6)−2.110(5) (2.070)	2.053(5)−2.133(5) (2.093)	2.056(7)−2.118(7) (2.087)
Fe−N_{py} (Å) (mean)	2.231(4), 2.170(5) (2.201)	2.197(6)−2.216(6) (2.205)	2.193(5)−2.215(5) (2.202)	2.175(4)−2.201(5) (2.192)	2.173(6)−2.2161(6) (2.197)
Fe−N_{amine} (Å) (mean)	2.230(4) (2.230)	2.254(6), 2.257(6) (2.256)	2.246(5), 2.250(5) (2.248)	2.239(4), 2.245(5) (2.242)	2.233(6), 2.248(6) (2.241)
Fe−N_{pym} (Å) (mean)	2.290(4) (2.290)	2.299(6), 2.299(6) (2.299)	2.298(5), 2.300(4) (2.299)	2.285(4), 2.287(4) (2.286)	2.433(6), 2.349(6) (2.391)
Fe···Fe (Å)[a]	6.626(2)	6.563(2)	6.574(1)	6.526(1)	6.782(1)
Fe−N_{All} (Å) (mean)	2.112(4)−2.290(4) (2.200)	2.025(7)−2.299(6) (2.184)	2.023(6)−2.300(4) (2.182)	2.053(5)−2.287(4) (2.183)	2.056(7)−2.433(6) (2.200)
cis N−Fe−N (mean)	75.2(2)−102.2(2) (90.0)	73.6(2)−120.8(2) (89.7)	73.9(2)−120.1(2) (89.7)	74.9(2)−120.0(2) (89.8)	70.4(2)−104.9(2) (89.8)
trans N−Fe−N (mean)	164.3(1)−176.7(2) (171.9)	148.8(2)−164.4(3) (157.9)	149.4(2)−165.0(2) (158.3)	150.0(2)−166.3(2) (159.2)	156.2(2)−171.5(3) (165.7)
Σ (deg) (mean)	50.1 (50.1)	118.4, 118.0 (118.2)	117.8, 115.6 (116.7)	104.3, 102.8 (103.6)	79.3, 80.8 (80.1)
Fe out of pyrimidine plane	+0.556, +0.556	+0.482, −0.531	+0.491, −0.502	+0.510, −0.524	+1.106, −1.325
π-stacking interactions:					
centroid ··· centroid (Å)		3.841−3.914	3.825−3.944	3.872−3.912	
mean plane···centroid (Å)		3.613−3.829	3.621−3.774	3.593−3.812	
offset angle (deg)		9.7−21.6	9.4−23.1	11.5−23.4	
E···E interactions (Å)[b]		3.663	3.651		

[a]Fe···Fe separation across the pyrimidine bridge. [b]E is S or Se.

Table 3. Summary of Magnetic and Mössbauer Parameters for the Nine Diiron(II) Complexes Synthesized in This Work

			magnetic parameters				Mössbauer parameters				
ligand	co-ligand	complex	H^a	J^b	g	μ_{eff}/Fe^f	δ^c	$\Delta E_Q{}^c$	$\Gamma_L{}^c$	$\Gamma_R{}^c$	T^d
L^{Et}	NCS	1·MeOH·$^3/_4H_2O$	$-J[S_1S_2]$	−1.40	2.05	4.98	1.14	2.40	0.61	0.52	4.8
	NCSe	2·H_2O	$-J[S_1S_2]$	−1.65	2.00	4.92	1.18	2.20	0.64	0.64	4.5
	$NCBH_3$	3·$^5/_2H_2O$	$-J[S_1S_2]$	−2.20	2.06	5.12					
L^{Me}	NCS	4·$^1/_2H_2O$	$-J[S_1S_2]$	−1.43	2.15	5.41	1.12	2.72	0.23	0.25	4.8
	NCSe	5	$-J[S_1S_2]$	−1.27	2.20	5.41	1.13	2.69	0.22	0.24	4.7
	$NCBH_3$	6·$^3/_2H_2O$	$-J[S_1S_2]$	−1.56	2.02	4.79	1.15[e]	2.30[e]			4.6
L^{Mix}	NCS	7·$^1/_2H_2O$	$-J[S_1S_2]$	−1.31	2.16	5.38	1.13	2.13	0.37	0.36	4.8
	NCSe	8·$^3/_2H_2O$	$-J[S_1S_2]$	−1.54	2.20	5.44	1.14	1.98	0.40	0.38	4.5
	$NCBH_3$	9·$^3/_2H_2O$	$-J[S_1S_2]$	−1.63	2.13	5.26	1.16[e]	2.05[e]			4.7

[a]Spin Hamiltonian used to fit the experimental data set. [b]Units cm^{-1}. [c]Units mm s^{-1}, Voigt line shape. [d]Units K. [e]raw data. [f]Units μ_B.

As described earlier, the degree of distortion from the ideal octahedral geometry decreases in the order Fe_2L^{Me} (Σ 102.8−118.4°) > Fe_2L^{Mix} (Σ 80.6°) > Fe_2L^{Et} (Σ 50.1°), albeit this must be taken with some caution as the anions are different. Studies have shown that minimal values of Σ are associated with strong crystal fields and hence stabilization of the LS state.[8,18,42,46] Thus, from the observed value it appears that complexes of L^{Et} are the most likely candidates to show SCO or LS behavior compared to the complexes of L^{Me} and L^{Mix} and also the related ligand L^2.

The Fe−N_{pym} distances largely determine the Fe···Fe separations across the pyrimidine bridge. These consequently follow the order 8·$^7/_{10}$MeOH [av. 2.391, 6.782(1) Å] > 3·DMF·MeCN·$^3/_5Et_2O$ > [2.290, 6.626(2) Å] > 4 [av. 2.299,

dx.doi.org/10.1021/ic3012052 | Inorg. Chem. 2012, 51, 9056−9065

6.563(2) Å] ≈ **5** [av. 2.299, 6.574(1) Å] > **6** [av. 2.286, 6.526(1) Å] (Table 2). This also explains why they are all longer than seen in $[Fe^{II}_2L^2(NCS)_4]$ [2.229, 6.288(1) Å].[10]

There are no intra/intermolecular π-ring stacking interactions in **3**·DMF·MeCN·$^3/_5Et_2O$ and **8**·$^7/_{10}$MeOH. However, in **4**–**6** the equatorial pyridine rings that are "*trans*" to each other are tilted toward the central pyrimidine plane. Consequently, there are offset parallel intramolecular interactions between the *trans* positioned pyridine and pyrimidine rings [N(14) and N(18) with N(11) pyrimidine ring, Table 2 and Supporting Information, Figures S1, S3, and S5]. There are also offset parallel weak intermolecular interactions between the pyridine rings [N(14) and N(17) of adjacent molecules] in **4**–**6** as well as S···S and Se···Se interactions in **4** and **5** (Supporting Information, Figures S1 and S3).[18,42] As no spin transition takes place in any of the complexes no statements can be made about the influence of these interactions on cooperativity.

Magnetochemistry and Mössbauer Spectroscopy. Variable temperature magnetic susceptibility measurements were made on powder samples of all nine complexes in the temperature range 300 to 2 K (for **2**–**8**) or 300 to 4 K (for **1**) (Table 3, Figure 5 and Supporting Information, Figure S6–S13). Least squares regression of the data to a modified Van Vleck equation, using MAGMUN 4.1,[47,48] was performed using the Hamiltonian $H = -J[\mathbf{S_1 \cdot S_2}]$, and corrected for intermolecular effects (θ, Weiss-like correction), the fraction of paramagnetic, Curie-like impurity (α), the temperature independent paramagnetism (TIP), and zero field splitting (ZFS).

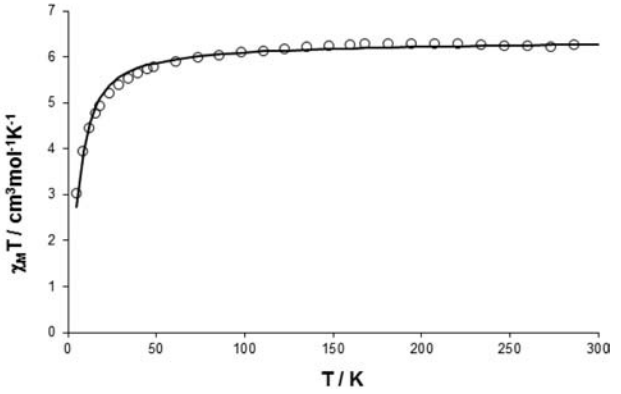

Figure 5. Plot of $\chi_M T$ versus temperature for **1**·MeOH·$^3/_4H_2O$. The solid line corresponds to the best fit.

In all cases the iron(II) centers were found to be stabilized in the [HS-HS] state across the entire experimental temperature range, and to exhibit weak antiferromagnetic coupling. For example, the plot of experimental $\chi_M T$, for **1**·MeOH·$^3/_4H_2O$ is shown in Figure 5. The $\chi_M T$ value at 300 K of 6.2 cm^3 mol^{-1} K (3.1 cm^3 mol^{-1} K per Fe^{II}, μ_{eff} = 7.08 μ_B, $\mu_{eff/Fe}$ = 4.98 μ_B) is in agreement with the expected spin only value of an iron(II) ion in the HS state (spin only $\chi_M T$ *for S = 2 is* 3.0 cm^3 mol^{-1} K). This value remains relatively constant until reaching 50 K; below this temperature the $\chi_M T$ value drops to 1.5 cm^3 mol^{-1} K at 4 K, because of ZFS. The best fit for this data set gave the following parameters $J = -1.3988 \pm 0.0058$ cm^{-1}, $g = 2.0483 \pm 0.0504$, TIP = 1.5×10^{-4} cm^3/mol, and $\alpha = 0.05$, $\theta = 0.25$ K ($10^2R = 1.65$) (Table 3). The eight other complexes, despite their differences in strain energy and coligands, show similar magnetic features (Table 3, Supporting Information, Figures S6–S13).

To probe the oxidation and spin states of the iron centers further, ^{57}Fe Mössbauer spectra were measured at low temperatures (4.4–4.8 K). Unfortunately, the samples were air sensitive and by the time the Mössbauer data was collected the aged magnetic sample of **3**·$^5/_2H_2O$ contained significant ferric impurities. Then, as noted earlier, attempts to repeat the clean preparation of that iron(II) sample failed, despite repeated attempts. Likewise, **1**·MeOH·$^3/_4H_2O$ contained very small amounts of a ferric impurity (Supporting Information, Figure S14).

The Mössbauer spectra of the eight complexes (i.e., all but **3**·$^5/_2H_2O$) proved that the iron(II) ions are indeed present in the [HS-HS] state, in perfect agreement with the magnetic and X-ray results (Table 3). All spectra provided parameters characteristic of HS iron(II), that is, $\delta \sim 1.1$ mm s^{-1} and $\Delta E_Q \sim 2$–3 mm s^{-1}.[43,49] The parameters were refined assuming initially symmetrical quadrupole doublets (equal line widths) with Voigt line shape. The spectra of the complexes are shown in Figure 6 and Supporting Information, Figures S14–S15.

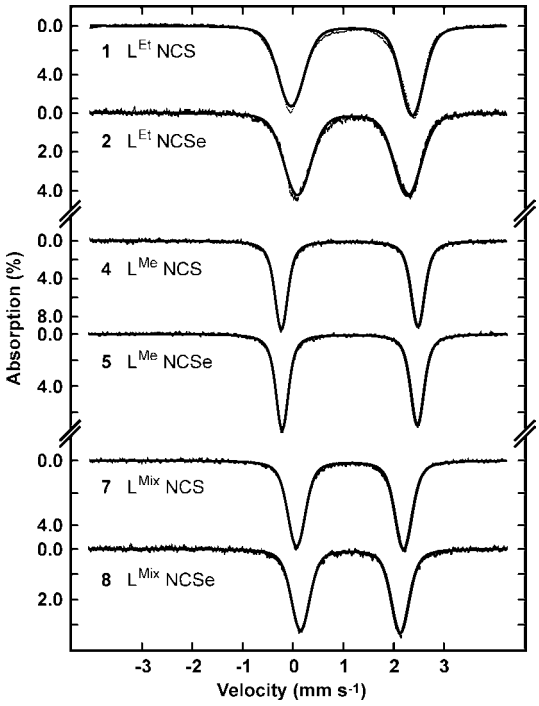

Figure 6. ^{57}Fe–Mössbauer spectra for all complexes with coligands NCS and NCSe.

Unfortunately it was not possible to fit the spectrum of **6**·$^3/_2H_2O$ or **9**·$^3/_2H_2O$ because of the broadness of the signal, nonethelesss the spectra are also consistent with the complexes being stabilized in the [HS-HS]-state.

In general, only those complexes with the ligand $\mathbf{L^{Me}}$ gave sharp quadrupole doublets. The $\mathbf{L^{Et}}$ samples and those with $NCBH_3$ as coligand are particularly broad, and this almost certainly arises from the powdery, noncrystalline nature of the samples caused by the use of diethyl ether to rapidly precipitate the complexes.

Some general trends in the Mössbauer parameters can be observed (Table 3). When the coligand NCS is replaced by

dx.doi.org/10.1021/ic3012052 | Inorg. Chem. 2012, 51, 9056–9065

Table 4. Crystal Structure Determination Details for $[Fe^{II}_2L^{Et}(NCBH_3)_4]\cdot DMF\cdot MeCN\cdot{}^3/_5Et_2O$ (3·DMF·MeCN·$^3/_5$Et$_2$O), $[Fe^{II}_2L^{Me}(NCS)_4]$ (4), $[Fe^{II}_2L^{Me}(NCSe)_4]$ (5), $[Fe^{II}_2L^{Me}(NCBH_3)_4]$ (6), $[Fe^{II}_2L^{Mix}(NCSe)_4]\cdot{}^7/_{10}MeOH$ (8·$^7/_{10}$MeOH)

	complex				
	3·DMF·MeCN·$^3/_5$Et$_2$O	4	5	6	8·$^7/_{10}$MeOH
formula	$C_{51.40}H_{70}B_4Fe_2N_{14}O_{1.60}$	$C_{40}H_{34}Fe_2N_{12}S_4$	$C_{40}H_{34}Fe_2N_{12}Se_4$	$C_{40}H_{46}B_4Fe_2N_{12}$	$C_{42.70}H_{40.80}Fe_2N_{12}O_{0.70}Se_4$
M_r	1064.55	922.73	1110.33	849.83	1160.81
crystal system	orthorhombic	monoclinic	monoclinic	monoclinic	monoclinic
space group	*Pnma*	$P2_1/n$	$P2_1/n$	$P2_1/n$	$P2_1/c$
a [Å]	24.399(2)	11.154(4)	11.2380(6)	11.1880(12)	9.3377(5)
b [Å]	22.286(1)	19.963(5)	20.3994(9)	20.594(3)	24.7012(13)
c [Å]	11.269(9)	18.506(4)	18.6755(10)	18.683(2)	19.9340(10)
α [deg]	90	90	90	90	90
β [deg]	90	99.121(1)	100.18(1)	99.41(1)	97.35(3)
γ [deg]	90	90	90	90	90
V [Å^3]	6127.6(7)	4068.4(2)	4214.0(4)	4246.9(8)	4560.0(4)
Z	4	4	4	4	4
$\rho_{calcd.}$[g/cm^3]	1.154	1.506	1.750	1.329	1.691
μ [mm^{-1}]	0.520	0.966	4.19	0.728	3.877
F(000)	2245	1896	2184	1768	2298
T [K]	92	92	91	91	91
θ range for data collection [deg]	2.46 to 26.45	2.23 to 25.41	2.28 to 23.02	2.22 to 24.45	2.35 to 22.08
reflections collected	84902	33031	46867	49291	48205
independent reflections	6447	7172	8621	8632	8696
R(int)	0.0744	0.1293	0.0964	0.1768	0.1037
T_{min}/T_{max}	0.757	0.005	0.713	0.829	0.583
data/restraints/parameters	6447/14/396	7172/189/523	8621/0/523	8632/0/527	8696/15/570
Gof (F^2)	1.070	1.132	1.021	1.018	1.035
$R1/wR2$ [$I > 2\sigma(I)$]	0.0765/0.2107	0.0988/0.1824	0.0535/0.1162	0.0718/0.1633	0.0610/0.1401
$R1/wR2$ (all data)	0.1061/0.2288	0.1424/0.1988	0.1050/0.1362	0.1612/0.2022	0.1405/0.1746
max. peak/hole [e Å^{-3}]	1.190/−0.806	1.118/−0.588	2.785/−1.676	0.518/−0.565	1.266/−1.456

NCSe or $NCBH_3$, there is an increase in the isomer shift (δ) and decrease in the quadrupole splitting (ΔE_Q). There is no obvious correlation between the Mössbauer and IR data (Table 1), but the trend in isomer shift can be explained when compared with the Fe−NCE bond distances (Table 2). The Fe−N_{NCE} bond distances follow the trend $NCBH_3$ > NCSe > NCS with an average of 2.116 > 2.079 > 2.068 Å. This relation between bond distance and isomer shift is experimentally known,[50] and theoretical investigations[51] have shown that longer Fe−N bond distances increase the isomer shift by relative elongation of the 3s- and 4s-iron orbitals.

The decrease in the quadrupole splitting can be related to the octahedral distortion (Σ). As Σ increases, so does the electric field gradient caused by the 3d crystal field and thus the quadrupole splitting also increases. On this basis, the ΔE_Q follows the order **6**·$^3/_2H_2O$ < **5** < **4**·$^1/_2H_2O$ (Table 3), and this is in good agreement with the mean distortion parameters Σ: **6** (103.6°) < **5** (116.7°) < **4** (118.2°), Table 2.

CONCLUSION

Nine dinuclear iron(II) complexes of three bis-*tetra*dentate pyrimidine-based ligands, L^{Et}, L^{Me}, and L^{Mix}, with three NCE coligands (E = S, Se, BH_3) have been successfully synthesized and characterized. Five complexes were structurally characterized. In all cases the iron(II) centers had distorted octahedral geometries with the degree of distortion varying in the order Fe_2L^{Me} > Fe_2L^{Mix} > Fe_2L^{Et}.

The variable temperature magnetic and Mössbauer results show that (a) weak antiferromagnetic coupling is a feature of all of them, with $-2.20 \le J \le -0.73$ cm^{-1}, and (b) they all remain in the [HS-HS] state down to 2 K. This shows that the pyrimidine-based ligands used in this study impose only a weak field on iron(II), such that even when used in combination with NCE (E = S, Se, BH_3) coligands the resulting complexes do not undergo SCO to the LS state. Use of cyanide coligands is an obvious way to increase the field further, but this possibility was not explored in the present study.

The observed significant distortions of the metal centers from an ideal octahedral geometry is a key factor that favors the [HS-HS] state and may prevent observation of the SCO effect.[8,18,42,46] Close inspection of these parameters in the present complexes indicates that complexes of L^{Et} are the most likely candidates to show SCO or LS behavior, compared to complexes of L^{Me} and L^{Mix}. Nevertheless, even with the strong field coligand $NCBH_3$, the complexes of L^{Et} were [HS-HS] down to 2 K.

It should also be noted that SCO depends on many factors, including the interplay between the ligand-field strength at the transition metal ion and the interactions between the metal complex, the counterions, and the solvate molecules, as governed by crystal packing. Thus, modifying the ligand by replacing the pyridimine ring phenyl substituent by one that facilitates strong intermolecular interactions (and preferably also increases the field strength), or use of a different heterocycle to increase communication across the bridge, may generate sufficient strength and cooperativity to give the desired SCO behavior, or at least the possibility of obtaining systems other than [HS-HS]. These aspects are the next focus of this research group.

dx.doi.org/10.1021/ic3012052 | *Inorg. Chem.* 2012, 51, 9056−9065

EXPERIMENTAL SECTION

General experimental information is provided in the Supporting Information. Crystal structure data is provided in Table 4 and the Supporting Information.

Where noted acetonitrile and methanol were refluxed over CaH_2 and Mg/I_2 prior to use, respectively, otherwise HPLC grade was used as received. 4,6-Bis(hydroxymethyl)-2-phenylpyrimidine (A) and $\mathbf{L^{Et}}$ were synthesized according to our previous report.[19] *N*-Bis(2-pyridylmethyl)amine (bmpa)[28,29] and *N*-(2-pyridylethyl)-*N*-(2′-pyridylmethyl)amine (pmpea)[30,31] were prepared according to the literature methods. $[Fe^{II}(NCE)_2(py)_4]$, E = S, Se, or BH_3, were made according to the published procedure.[32] All other chemicals and solvents were of reagent grade and were used as received.

4,6-Bis(chloromethyl)-2-phenylpyrimidine (C). To a pale yellow solution of 4,6-bis(hydroxymethyl)-2-phenylpyrimidine (A) (1.0 g, 5.0 mmol) in CH_2Cl_2, under nitrogen, was added $SOCl_2$ (0.75 mL, 10 mmol). The resulting deep yellow suspension was stirred for 1 h before the solvent was removed by blowing nitrogen over it and further dried under vacuum to give pure 4,6-bis(chloromethyl)-2-phenylpyrimidine as an orange solid in a quantitative yield. Found: C, 56.70; H, 4.15; N, 10.84 $C_{12}H_{10}N_2Cl_2$ (253.13 g mol^{-1}) requires: C, 56.94; H, 3.98; N, 11.07. δ_H (300 MHz, solvent $CDCl_3$, reference $CHCl_3$ @ 7.26 ppm): 8.52 ($2H_{2'}$, m), 7.71 (H_5, s), 7.52 ($2H_{3'}$ & $H_{4'}$, m), 4.76 ($4H_7$, s). δ_C (125 MHz, solvent $CDCl_3$, reference $CHCl_3$ @ 77.3 ppm): 166.5 (C_2), 164.3 (C_1), 136.8 ($C_{1'}$), 131.3 ($C_{4'}$), 128.8 ($C_{3'}$), 128.6 ($C_{2'}$), 115.1 (C_5), 45.7 (C_7). ESI-MS(+) ($CHCl_3$-MeOH *m*/*z*): $[C_{12}H_{10}N_2Cl_2 + H]^+$ requires 253.0294, found 253.0276. IR (KBr, cm^{-1}): 3312, 1630, 1588, 1573, 1546, 1455, 1409, 1379, 1302, 1260, 1169, 1120, 1066, 1024, 933, 739, 720, 693, 685, 640, 560.

4,6-Bis[*N*,*N*-bis(2′-pyridylmethyl)aminomethyl]-2-phenyl pyrimidine ($\mathbf{L^{Me}}$). To a mixture of 4,6-bis(chloromethyl)-2-phenyl-pyrimidine (0.05 g, 0.2 mmol) and excess of Na_2CO_3 (0.42 g, 4 mmol) in 50 mL of acetonitrile was added a solution of bmpa (0.08 g, 0.4 mmol), and a catalytic amount of KI. The reaction mixture was refluxed overnight. The insoluble solid was filtered off and the filtrate taken to dryness to give a red brown oil. The brown oil was dissolved in H_2O (20 mL) and extracted with CH_2Cl_2 (3 × 50 mL). The combined organic phase was dried over $MgSO_4$, filtered, and taken to dryness to afford $\mathbf{L^{Me}}$ in 95% yield. Found: C, 74.43; H, 6.01; N, 19.31 $C_{36}H_{34}N_8$ (578.71 g mol^{-1}) requires: C, 74.72; H, 5.92; N, 19.36. δ_H (500 MHz, solvent $CDCl_3$, reference $CHCl_3$ @ 7.26 ppm): 8.53 ($4H_{14}$, ddd), 8.43 ($2H_{2'}$, m), 7.89 (H_5, s), 7.67 ($4H_{11}$, d), 7.56 ($2H_{12}$, td), 7.43 ($2H_{3'}$ & $1H_{4'}$, m), 7.14 ($4H_{13}$, ddd), 3.99 ($8H_9$, s), 3.96 ($4H_7$, s). δ_C (125 MHz, solvent $CDCl_3$, reference $CHCl_3$ @ 77.3 ppm): 168.41 (C_4), 163.91 ($C_{1'}$), 158.72 (C_{10}), 149.02 (C_{14}), 137.76 (C_2), 136.78 (C_{11}), 130.58 ($C_{4'}$), 128.48 ($C_{3'}$), 128.33 ($C_{2'}$), 123.09 (C_{12}), 122.34 (C_{13}), 115.82 (C_5), 60.2 (C_9), 59.5 (C_7). ESI-MS(+) ($CHCl_3$ *m*/*z*): $[\mathbf{L^{Me}}H]^+$ requires 579.2979, found 579.3026; $[\mathbf{L^{Me}}Na]^+$ requires 601.2801, found 601.2842. IR (KBr, cm^{-1}): 3068, 3007, 2916, 2816, 1588, 1569, 1542, 1470, 1436, 1379, 1249, 1146, 1043, 994, 761, 689. λ_{max}/nm (ε/dm^3 mol^{-1} cm^{-1}) [CH_3CN] = 259 (27000).

4,6-[(2′-Pyridylmethyl)-2′-pyridylethyl)aminomethyl]-2-phenylpyrimidine ($\mathbf{L^{Mix}}$). To a mixture of pmpea (2.89 g, 13.6 mmol) and 4,6-bis(chloromethyl)-2-phenylpyrimidine (1.78 g, 6.78 mmol) in 150 mL of warm freshly distilled acetonitrile was added an excess of Na_2CO_3 (5.75 g, 54.2 mmol) and a catalytic amount of KI. The reaction mixture was refluxed overnight. After cooling to room temperature, the insoluble solid was filtered off, and the filtrate was taken to dryness under reduced pressure. The resulting brown oil was then purified by column chromatography on alumina using ethyl acetate as eluent to give $\mathbf{L^{Mix}}$ as orange brown oil in 75% yield. TLC: $R_{F(product)}$ = 0.60. Found: C, 73.23; H, 6.31; N, 17.71. $C_{38}H_{38}N_8{\cdot}H_2O$ (624.78 g mol^{-1}) requires: C, 73.05 H, 6.45; N, 17.93. δ_H (400 MHz, solvent $CDCl_3$, reference $CHCl_3$ @ 7.26 ppm): 8.52−8.44 ($2H_{14'}$, $2H_{2'}$ & $2H_{14}$, m), 7.51−7.44 ($2H_{12}$, H_5, $2H_{12'}$, $H_{4'}$ & $2H_{3'}$, m), 7.37 ($2H_{11'}$, d), 7.17−7.06 ($2H_{11}$, $2H_{13}$ & $2H_{13'}$), 3.94 ($4H_7$, s), 3.91 ($4H_{9'}$, s), 3.05 ($4H_8$ & $4H_9$, m). δ_C (100 MHz, solvent, $CDCl_3$, reference $CHCl_3$ @ 77.3 ppm): 168.9 (C_4), 163.85 (C_2), 160.3 ($C_{10'}$), 159.7 (C_{10}), 149.3 ($C_{14'}$), 149.1 (C_{14}), 138.0 ($C_{1'}$), 136.5 ($C_{4'}$), 136.3 ($C_{12'}$), 130.5 (C_{12}), 128.5 ($C_{3'}$), 128.4 ($C_{2'}$), 123.5 (C_{11}), 122.8 ($C_{11'}$), 122.1 (C_{13}), 121.3 ($C_{13'}$), 116.2 (C_5), 60.7 (C_7), 59.6($C_{9'}$), 54.7 (C_8), 36.2 (C_9). ESI-MS(+) (MeOH *m*/*z*): $[\mathbf{L^{Mix}}H]^+$ requires 607.3292 found 607.3265. IR (KBr, cm^{-1}): 3061, 3007, 2928, 2822, 1638, 1588, 1568, 1542, 1473, 1432, 1374, 1251, 1146, 1047, 1027, 992, 749, 694, 613, 402. λ_{max}/nm (ε/dm^3 mol^{-1} cm^{-1}) [CH_3CN] = 258 (28500).

$[Fe^{II}_2\mathbf{L^{Et}}(NCS)_4]{\cdot}MeOH{\cdot}{}^3/_4H_2O$ ($1{\cdot}MeOH{\cdot}{}^3/_4H_2O$). To a refluxing yellow solution of $\mathbf{L^{Et}}$ (0.07 g, 0.11 mmol) in MeOH (3 mL) was added a pale yellow solution $[Fe^{II}(NCS)_2(Py)_4]$ (0.11 g, 0.22 mmol) in MeOH (10 mL), all under argon, leading to an orange solution. After 3 h the orange solution was cooled to room temperature followed by dropwise addition of degassed diethyl ether (∼ 60 mL), via cannula, resulting in the precipitation of an orange solid. The mixture was left to stand for 1 h, and then the orange solid was filtered off and dried under vacuum (0.09 g, 80%). Found: C, 52.18; H, 4.38; N, 16.11; S, 11.96. $[Fe^{II}_2\mathbf{L^{Et}}(NCS)_4]{\cdot}MeOH{\cdot}{}^3/_4H_2O$ (1024.89 g/mol) requires C, 52.76; H, 4.67; N, 16.41; S, 12.52. ESI-MS(+) (MeOH *m*/*z*): $[\mathbf{L^{Et}}H]^+$ requires 635.3605 found 635.3698; $[Fe^{II}\mathbf{L^{Et}}(NCS)]^+$ requires 748.2629 found 748.2619; $[Fe^{II}_2\mathbf{L^{Et}}(NCS)_3]^+$ requires 920.1482 found 920.1415. IR (KBr, cm^{-1}): 3412, 2038, 1588, 1569, 1546, 1474, 1436, 1379, 1215, 1146, 1036, 1001, 754, 693, 628, 480.

$[Fe^{II}_2\mathbf{L^{Et}}(NCSe)_4]{\cdot}H_2O$ ($2{\cdot}H_2O$). To a yellow solution of $\mathbf{L^{Et}}$ (0.07 g, 0.11 mmol) in MeOH (10 mL) under reflux was added a pale yellow solution of $[Fe^{II}(NCSe)_2(Py)_4]$ (0.13 g, 0.22 mmol) in MeOH (10 mL), all under argon. The resulting yellow reaction solution was refluxed for 1 h. After cooling to room temperature, degassed diethyl ether (∼ 60 mL) was added dropwise using a cannula leading to a precipitation of a yellow solid. The mixture was left to stand for 1 h before the yellow solid was filtered off and dried under vacuum (0.11 g, 85%). Found: C, 44.87; H, 3.65; N, 13.79. $[Fe^{II}_2\mathbf{L^{Et}}(NCSe)_4]{\cdot}H_2O$ (1184.45 g mol^{-1}) requires: C, 44.62; H, 3.74; N, 14.19. ESI-MS(+) (CH_3CN *m*/*z*): $[\mathbf{L^{Et}}H]^+$ requires 635.3605 found 635.3639; $[Fe^{II}\mathbf{L^{Et}}(NCSe)]^+$ requires 796.2077 found 796.2071; $[Fe^{II}_2\mathbf{L^{Et}}(NCSe)_3]^+$ requires 1063.9832 found 1063.9826; $[Fe^{II}_2\mathbf{L^{Et}}(NCSe)_4K]^+$ requires 1208.8670 found 1208.8671. IR (KBr, cm^{-1}): 3435, 3061, 2916, 2847, 2061, 1600, 1565, 1542, 1478, 1436, 1382, 1314, 1154, 1104, 1059, 1028, 948, 780, 754, 697, 643, 419.

$[Fe^{II}_2\mathbf{L^{Et}}(NCBH_3)_4]{\cdot}{}^5/_2H_2O$ ($3{\cdot}{}^5/_2H_2O$). To a refluxing suspension of $[Fe^{II}(NCBH_3)_2(Py)_4]$ (0.14 g, 0.30 mmol) in MeCN (∼10 mL) was added a yellow solution of $\mathbf{L^{Et}}$ (0.10 g, 0.15 mmol) in MeCN (∼10 mL), all under argon. All the solids dissolved within about 10 min. After 1 h the solution was cooled to room temperature followed by addition of degassed diethyl ether (∼ 70 mL) using a cannula, resulting in the precipitation of a yellow solid. The yellow solid was filtered off and dried under vacuum (0.14 g, 91%). Found: C, 56.04; H, 6.03; N, 17.18. $[Fe^{II}_2\mathbf{L^{Et}}(NCBH_3)_4]{\cdot}{}^5/_2H_2O$ (950.95 g mol^{-1}) requires: C, 55.57; H, 6.25; N, 17.67. ESI-MS(+) (DMF-MeOH *m*/*z*): $[\mathbf{L^{Et}}H]^+$ requires 635.3605 found 635.3639; $[\mathbf{L^{Et}}Na]^+$ requires 657.3425 found 657.3383 $[Fe^{II}\mathbf{L^{Et}}(NCBH_3)]^+$ requires 730.3243 found 730.3196; $[Fe^{II}_2\mathbf{L^{Et}}(NCBH_3)_3]^+$ requires 866.3323 found 866.3219. IR (KBr, cm^{-1}): 3448, 3064, 2931, 2862, 2334, 2182, 1601, 1564, 1545, 1481, 1439, 1388, 1319, 1154, 1115, 1063, 1019, 950, 756, 697, 640, 419.

$[Fe^{II}_2\mathbf{L^{Me}}(NCS)_4]{\cdot}{}^1/_2H_2O$ ($4{\cdot}{}^1/_2H_2O$). To a refluxing yellow solution of $\mathbf{L^{Me}}$ (0.05 g, 0.08 mmol) in MeCN (20 mL), was added 10 mL of a yellow solution of $[Fe^{II}(NCS)_2(Py)_4]$ (0.08 g, 0.16 mmol), all under argon, initially resulting in a red solution that turn to a suspension in a few minutes (∼10 min). The suspension was refluxed for 2 h before it was cooled down to room temperature. The brick red solid obtained was then filtered off and dried under vacuum (0.06 g, 80%). Found: C, 51.40; H, 3.68; N, 18.18; S, 13.30. $[Fe_2\mathbf{L^{Me}}(NCS)_4]{\cdot}{}^1/_2H_2O$ (931.74 g mol^{-1}) requires: C, 51.56; H, 3.79; N, 18.04; S, 13.76. ESI-MS(+) (DMF-MeOH *m*/*z*): $[\mathbf{L^{Me}}H]^+$ requires 579.2979 found 579.3026; $[\mathbf{L^{Me}}Na]^+$ requires 601.2799 found 601.2840; $[Fe^{II}\mathbf{L^{Me}}(NCS)]^+$ requires 692.2002 found 692.2037; $[Fe^{II}_2\mathbf{L^{Me}}(NCS)_3]^+$ requires 864.0856 found 864.0963. IR (KBr, cm^{-1}): 3345, 3068, 2926, 2068, 1599, 1569, 1545, 1474, 1434, 1392, 1343, 1287, 1154, 1095, 1048, 1011, 908,781, 761, 702, 648.

$[Fe^{II}_2\mathbf{L^{Me}}(NCSe)_4]$ (5). To a refluxing yellow solution of $\mathbf{L^{Me}}$ (0.07 g, 0.11 mmol) in MeOH (10 mL), was added 10 mL of a yellow solution of $[Fe^{II}(NCSe)_2(Py)_4]$ (0.13 g, 0.22 mmol) in MeOH, all under argon,

dx.doi.org/10.1021/ic3012052 | *Inorg. Chem.* 2012, 51, 9056−9065

affording a reddish suspension in a few minutes (~10 min). The suspension was refluxed for 1 h before it was cooled down to room temperature. The brick red solid was then filtered off and dried under vacuum (0.10 g, 82%). Found: C, 43.19; H, 3.12; N, 15.03; $[Fe^{II}_2L^{Me}(NCSe)_4]$ (1110.31 g mol^{-1}) requires: C, 43.27; H, 3.09; N, 15.14. ESI-MS(+) (DMF-MeOH *m*/*z*): $[L^{Me}H]^+$ requires 579.2979 found 579.2817; $[L^{Me}Na]^+$ requires 601.2799 found 601.2647; $[Fe^{II}L^{Me}(NCSe)]^+$ requires 740.1451 found 740.1240; $[Fe^{II}_2L^{Me}(NCSe)_3]^+$ requires 1007.9214 found 1007. 8961. IR (ATR, cm^{-1}): 2053, 1600, 1569, 1544, 1477, 1438, 1414, 1393, 1346, 1287, 1155, 1096, 1049, 1014, 946, 908.

$[Fe^{II}_2L^{Me}(NCBH_3)_4]\cdot{}^3/_2H_2O$ ($6\cdot{}^3/_2H_2O$). To a refluxing suspension of $Fe^{II}(NCBH_3)_2(Py)_4$ (0.09 g, 0.20 mmol) in MeCN (10 mL), was added a yellow solution of L^{Me} (0.06 g, 0.10 mmol) in MeCN (8 mL), all under argon, resulting in a clear orange red solution after a few minutes (~10 min). After the reaction solution was refluxed for 3 h, and cooled down to room temperature, degassed diethyl ether (~ 75 mL) was slowly added using a cannula to give a yellow suspension. The suspension was left to stand for 1 h at room temperature before the yellow solid was filtered off and dried under vacuum (0.75 g, 92%). Found: C, 54.63; H, 5.42; N, 19.69. $[Fe^{II}_2L^{Me}(NCBH_3)_4]\cdot{}^3/_2H_2O$ (833.59 g mol^{-1}) requires: C, 54.79; H, 5.63; N, 19.17. ESI-MS(+) (DMF-MeOH *m*/*z*): $[L^{Me}H]^+$ requires 579.2979 found 579.2956; $[L^{Me}Na]^+$ requires 601.2799 found 601.2795; $[Fe^{II}L^{Me}(NCBH_3)(H_2O)]^+$ requires 692.2722 found 692.1994; $[Fe^{II}L^{Me}(NCBH_3)]^+$ requires 674.2616 found 674.2530; $[Fe^{II}_2L^{Me}(NCBH_3)_3]^+$ requires 810.2696 found 810.1628. IR (KBr, cm^{-1}): 3433, 3068, 2926, 2339, 2177, 1599, 1567, 1545, 1478, 1439, 1395, 1343, 1287, 1115, 1051, 1014, 903, 761, 692, 645.

$[Fe^{II}_2L^{Mix}(NCS)_4]\cdot{}^1/_2H_2O$ ($7\cdot{}^1/_2H_2O$). To a refluxing yellow solution of L^{Mix} (0.06 g, 0.09 mmol) in MeOH (10 mL), was added a yellow solution of $[Fe^{II}(NCS)_2(Py)_4]$ (0.09 g, 0.18 mmol) in MeOH (10 mL) gradually resulting in a yellow suspension (~ 5−10 min). The yellow suspension was further refluxed for 2 h before it was cooled down to room temperature. The yellow solid was then filtered off and dried under vacuum (0.05 g, 58%). Found: C, 52.60; H, 4.12; N, 17.29; S, 12.67. $[Fe^{II}_2L^{Mix}(NCS)_4]\cdot{}^1/_2H_2O$ (959.79 g mol^{-1}) requires: C, 52.56; H, 4.10; N, 17.51; S, 13.36. ESI-MS(+) (DMF-MeOH *m*/*z*): $[L^{Mix}H]^+$ requires 607.3292 found 607.3265; $[Fe^{II}L^{Mix}(NCS)]^+$ requires 720.2316 found 720.2316; $[Fe^{II}_2L^{Mix}(NCS)_3]^+$ requires 892.1169 found 892.1141. IR (KBr, cm^{-1}): 3433, 3064, 2845, 2866, 2068, 1596, 1537, 1481, 1439, 1388, 1301, 1154, 1009, 827,761, 741, 692.

$[Fe^{II}_2L^{Mix}(NCSe)_4]\cdot{}^3/_2H_2O$ ($8\cdot{}^3/_2H_2O$). To a refluxing yellow solution of L^{Mix} (0.07 g, 0.11 mmol) in MeOH (10 mL), was added 10 mL of a yellow solution of $[Fe^{II}(NCSe)_2(Py)_4]$ (0.13 g, 0.22 mmol) in MeOH, all under argon, affording a yellow suspension in a few minutes (~3−5 min). After the reaction mixture was refluxed for 1 h, the yellow solid was filtered off and dried under vacuum (0.11 g, 79%). Found: C, 43.25; H, 3.39; N, 14.15; $[Fe^{II}_2L^{Mix}(NCSe)_4]\cdot{}^3/_2H_2O$ (1165.38 g mol^{-1}) requires: C, 43.29; H, 3.55; N, 14.42. ESI-MS(+) (DMF-MeOH *m*/*z*): $[Fe^{II}_2L^{Mix}(NCSe)_3]^+$ requires 1033.9528 found 1035.9345; $[Fe^{II}L^{Mix}(NCSe)]^+$ requires 768.1764 found 768.1613; $[L^{Mix}H]^+$ requires 607.3292, found 607.3186. IR (KBr, cm^{-1}): 3433, 3064, 2931, 2857, 2064, 1601, 1569, 1537, 1483, 1442, 1400, 1390, 1306, 1267, 1156, 1102, 1083, 1048, 1016, 975, 913, 830, 761, 746, 690, 645, 586, 417.

$[Fe^{II}_2L^{Mix}(NCBH_3)_4]\cdot{}^3/_2H_2O$ ($9\cdot{}^3/_2H_2O$). To a refluxing suspension of $Fe^{II}(NCBH_3)_2(Py)_4$ (0.10 g, 0.22 mmol) in MeCN (10 mL), was added a yellow solution of L^{Mix} (0.07 g, 0.11 mmol) in MeCN (10 mL). All the solids dissolved within about 10 min. After 2 h the solution was cooled down to room temperature and subsequently degassed diethyl ether (~ 60 mL) was added using a cannula resulting in a yellow precipitate. After the mixture was left to stand overnight under argon, the yellow solid was filtered off and dried under vacuum (0.09 g, 90%). Found: C, 55.92; H, 5.93; N, 18.52; $[Fe^{II}_2L^{Mix}(NCBH_3)_4]\cdot{}^3/_2H_2O$ (904.88 g mol^{-1}) requires: C, 55.75; H, 5.90; N, 18.57. ESI-MS(+) (MeCN-MeOH *m*/*z*): $[L^{Mix}H]^+$ requires 607.3292 found 607.3264; $[Fe^{II}L^{Mix}(NCBH_3)]^+$ requires 702.2929 found 702.2890; $[Fe^{II}_2L^{Mix}(NCBH_3)_3]^+$ requires 838.3010 found 838.2928. IR (KBr, cm^{-1}): 3458, 3064, 2935, 2857, 2334, 2187, 1604, 1569, 1542, 1481, 1444, 1390, 1301, 1154, 1115, 1016, 758, 692, 631, 417.

■ ASSOCIATED CONTENT

Ⓢ Supporting Information

Includes details on instrumentation and measurements, details of structure determinations and disorder modeling, additional bond length and angle information, packing interaction figures and additional structure figures. Also additional magnetic and Mössbauer plots and a figure of **bmpa** and **pmpea**. This material is available free of charge via the Internet at http://pubs.acs.org. Supplementary crystallographic data can be obtained from the CCDC using the following reference codes: CCDC 856975−856979. This data can be obtained free of charge from the Cambridge Crystallographic Data Centre via www.ccdc.cam.ac.uk/data_request/cif.

■ AUTHOR INFORMATION

Corresponding Author

*E-mail: sbrooker@chemistry.otago.ac.nz.

Notes

The authors declare no competing financial interest.

■ ACKNOWLEDGMENTS

We are grateful to the University of Otago (Postgraduate Scholarship and Publishing Bursary to W.A.G.), the MacDiarmid Institute, and the Marsden Fund for funding this research. We thank Prof. Keith S. Murray and Dr. Boujemaa Moubaraki (Monash University) for the magnetic measurements on $1\cdot MeOH\cdot{}^3/_4H_2O$ and helpful suggestions, and Mrs. Marianne Dick and Mr. Bob McAllister (Campbell Microanalytical Laboratory, University of Otago) for the microanalyses.

■ REFERENCES

(1) Kahn, O.; Martinez, C. J. *Science* **1998**, *279*, 44−48.
(2) Létard, J.-F.; Guionneau, P.; Goux-Capes, L. *Top. Curr. Chem.* **2004**, *234*, 221−250.
(3) Klingele, M. H.; Moubaraki, B.; Cashion, J. D.; Murray, K. S.; Brooker, S. *Chem. Commun.* **2005**, 987−989.
(4) Grunert, C. M.; Reiman, S.; Spiering, H.; Kitchen, J. A.; Brooker, S.; Gütlich, P. *Angew. Chem., Int. Ed.* **2008**, *47*, 2997−2999.
(5) Brooker, S.; Plieger, P. G.; Moubaraki, B.; Murray, K. S. *Angew. Chem., Int. Ed.* **1999**, *38*, 408−410 and front cover feature..
(6) Klingele, M. H.; Moubaraki, B.; Murray, K. S.; Brooker, S. *Chem.—Eur. J.* **2005**, *11*, 6962−6973.
(7) Bhattacharjee, A.; Ksenofontov, V.; Kitchen, J. A.; White, N. G.; Brooker, S.; Gütlich, P. *Appl. Phys. Lett.* **2008**, *92*, 174104.
(8) Kitchen, J. A.; White, N. G.; Jameson, G. N. L.; Tallon, J. L.; Brooker, S. *Inorg. Chem.* **2011**, *50*, 4586−4597.
(9) Olguín, J.; Jameson, G. N. L.; Brooker, S. *Dalton Trans.* **2011**, *40*, 5086−5089.
(10) Oshio, H.; Ichida, H. *J. Phys. Chem.* **1995**, *99*, 3294−3302.
(11) Real, J. A.; Zarembowitch, J.; Kahn, O.; Solans, X. *Inorg. Chem.* **1987**, *26*, 2939−2943.
(12) Real, J. A.; Bolvin, H.; Bousseksou, A.; Dworkin, A.; Kahn, O.; Varret, F.; Zarembowitch, J. *J. Am. Chem. Soc.* **1992**, *114*, 4650.
(13) Andrés, E.; de Munno, G.; Julve, M.; Real, J. A.; Lloret, F. *J. Chem. Soc., Dalton Trans.* **1993**, 2169.
(14) Létard, J.-F.; Real, J. A.; Moliner, N.; Gaspar, A. B.; Capes, L.; Cador, O.; Kahn, O. *J. Am. Chem. Soc.* **1999**, *121*, 10630−10631.
(15) Breuning, E.; Ruben, M.; Lehn, J.-M.; Renz, F.; Garcia, Y.; Ksenofontov, V.; Gütlich, P.; Wegelius, E.; Rissanen, K. *Angew. Chem., Int. Ed.* **2000**, *39*, 2504−2507.

(16) Gaspar, A. B.; Ksenofontov, V.; Reiman, S.; Gütlich, P.; Thompson, A. L.; Goeta, A. E.; Muñoz, M. C.; Real, J. A. *Chem.—Eur. J.* **2006**, *12*, 9289−9298.
(17) Matouzenko, G. S.; Perrin, M.; Guennic, B. L.; Genre, C.; Molnar, G.; Bousseksou, A.; Borshch, S. A. *Dalton Trans.* **2007**, 934−942.
(18) Neville, S. M.; Leita, B., A.; Halder, G. J.; Kepert, C. J.; Moubaraki, B.; Letard, J.-F.; Murray, K. S. *Chem.—Eur. J.* **2008**, *14*, 10123−10133.
(19) Gobeze, W. A.; Milway, V. A.; Moubaraki, B.; Murray, K. S.; Brooker, S. *Dalton Trans.* **2012**, *41*, 9708−9721; Lan, Y. PhD Thesis, University of Otago, New Zealand, 2004.
(20) Ruben, M.; Breuning, E.; Lehn, J.-M.; Ksenofontov, V.; Renz, F.; Gütlich, P.; Vaughan, G. B. M. *Chem.—Eur. J.* **2003**, *9*, 4422−4429.
(21) Wilson, L. J.; Georges, D.; Hoselton, M. A. *Inorg. Chem.* **1975**, *14*, 2968−2975.
(22) Toftlund, H.; Yde-Andersen, S. *Acta Chem. Scand.* **1981**, *A35*, 575−585.
(23) Toftlund, H. *Coord. Chem. Rev.* **1989**, *94*, 67−108.
(24) Gaspar, A. B.; Ksenofontov, V.; Martinez, V.; Muñoz, M. C.; Real, J. A.; Gütlich, P. *Eur. J. Inorg. Chem.* **2004**, 4770−4773.
(25) Murray, K. S.; Kepert, C. J. *Top. Curr. Chem.* **2004**, *233*, 195−228.
(26) Gaspar, A. B.; Muñoz, M. C.; Real, J. A. *J. Mater. Chem.* **2006**, *16*, 2522−2533.
(27) Schneider, C. J.; Cashion, J. D.; Moubaraki, B.; Neville, S. M.; Batten, S. R.; Turner, D. R.; Murray, K. S. *Polyhedron* **2007**, *26*, 1764−1772.
(28) Neves, A.; de Brito, M. A.; Drago, V.; Griesar, K.; Haase, W. *Inorg. Chim. Acta* **1995**, *237*, 131−135.
(29) Carvalho, N. M. F.; Horn, A., Jr.; Bortoluzzi, A. J.; Drago, V.; Antunes, O. A. C. *Inorg. Chim. Acta* **2006**, *359* (1), 90−98.
(30) Rojas, D.; García, A. M.; Vega, A.; Moreno, Y.; Venegas-Yazigi, D.; Garland, M. T.; Manzur, J. *Inorg. Chem.* **2004**, *43*, 6324−6330.
(31) Romary, J. K.; Zachariasen, R. D.; Barger, J. D.; Schiesser, H. *J. Chem. Soc. (C)* **1968**, 2884.
(32) Kaufmann, G. B.; Alberts, R. A.; Harlan, F. L. *Inorg. Synth.* **1970**, *12*, 251.
(33) Ortega-Villar, N. A.; Muñoz, M. C.; Real, J. A. *Eur. J. Inorg. Chem.* **2010**, 5563−5567.
(34) Kitchen, J. A.; White, N. G.; Gandolfi, C.; Albrecht, M.; Jameson, G. N. L.; Tallon, J. L.; Brooker, S. *Chem. Commun.* **2010**, *46*, 6464−6466.
(35) Zhu, D.; Xu, Y.; Yu, Z.; Guo, Z.; Sang, H.; Liu, T.; You, X. *Chem. Mater.* **2002**, *14*, 838−843.
(36) Zhu, S.; Brennessel, W. W.; Harrison, R. G.; Que, L., Jr. *Inorg. Chim. Acta* **2002**, *337*, 32−38.
(37) Nakamoto, K., *Infrared and Raman Spectra of Inorganic and Coordination Compounds*, 3rd ed.; Wiley: New York, 1978.
(38) Youngme, S.; Phatchimkun, J.; Suksangpanya, U.; Pakawatchai, C.; van Albada, G. A.; Quesada, M.; Reedijk, J. *Inorg. Chem. Commun.* **2006**, *9*, 242−247.
(39) Liu, F.-C.; Chen, J.-H.; She, J.-J.; Lee, G.-H.; Peng, S.-M. *J. Organomet. Chem.* **2006**, *691*, 3574−3580.
(40) Baba, H.; Nakano, M. *Polyhedron* **2009**, *28*, 2087−2091.
(41) Hedelt, R.; Schulzke, C.; Rehder, D. *Inorg. Chem. Commun.* **2000**, *3*, 300−302.
(42) Amoore, J. J. M.; Kepert, C. J.; Cashion, J. D.; Moubaraki, B.; Neville, S. M.; Murray, K. S. *Chem.—Eur. J.* **2006**, *12*, 8220−8227.
(43) Gütlich, P.; Garcia, Y.; Goodwin, H. A. *Chem. Soc. Rev.* **2000**, *29*, 419−427.
(44) Drew, M. G. B.; Harding, C. J.; McKee, V.; Morgan, G. G.; Nelson, J. *J. Chem. Soc., Chem. Commun.* **1995**, 1035−1038.
(45) Deeney, F. A.; Charles, J. H.; Morgan, G. G.; McKee, V.; Nelson, J.; Teat, S. J.; Clegg, W. *J. Chem. Soc., Dalton Trans.* **1998**, 1837−1843.
(46) Matouzenko, G. S.; Jeanneau, E.; Verat, A. Y.; Bousseksou, A. *Dalton Trans.* **2011**, *40*, 9608−9618.
(47) Jotham, R. W.; Kettle, S. F. A. *Inorg. Chim. Acta* **1970**, *4* (1), 145−149.
(48) Thompson, L. K.; Waldmann, O.; Xu, Z. *Coord. Chem. Rev.* **2005**, *249*, 2677−2690 ; MAGMUN4.11/OW01.exe is available as a combined package free of charge from the authors (http://www.ucs.mun.ca/~lthomp/magmun). MAGMUN was developed by Dr. Zhiqiang Xu (Memorial University), and OW01.exe by Dr. O.Waldmann. We do not distribute the source codes. The origin of the programs should be quoted.
(49) Greenwood, N. N.; Gibb, T. C. *Mössbauer Spectroscopy*; Chapman and Hall Ltd: London, U.K., 1971; p 659.
(50) Gütlich, P.; Bill, E.; Trautwein, A. X. *Mössbauer Spectroscopy and Transition Metal Chemistry*; Springer-Verlag: Berlin, Germany, 2011.
(51) Neese, F. *Inorg. Chim. Acta* **2002**, *337*, 181−192.